ARMY RESEARCH LABORATORY

Experimental and Modeling Studies of Plasma Injection by an Electrothermal Igniter Into a Solid Propellant Gun Charge

by Michael J. Nusca and Stephen L. Howard

ARL-TR-3806 **June 2006**

NOTICES

Disclaimers

The findings in this report are not to be construed as an official Department of the Army position unless so designated by other authorized documents.

Citation of manufacturer's or trade names does not constitute an official endorsement or approval of the use thereof.

Destroy this report when it is no longer needed. Do not return it to the originator.

Army Research Laboratory
Aberdeen Proving Ground, MD 21005-5066

ARL-TR-3806 **June 2006**

Experimental and Modeling Studies of Plasma Injection by an Electrothermal Igniter Into a Solid Propellant Gun Charge

Michael J. Nusca and Stephen L. Howard
Weapons and Materials Research Directorate, ARL

REPORT DOCUMENTATION PAGE

Form Approved
OMB No. 0704-0188

1. REPORT DATE *(DD-MM-YYYY)*	2. REPORT TYPE	3. DATES COVERED (From - To)
June 2006	Final	June 2005–December 2005

4. TITLE AND SUBTITLE
Experimental and Modeling Studies of Plasma Injection by an Electrothermal Igniter Into a Solid Propellant Gun Charge

5a. CONTRACT NUMBER

5b. GRANT NUMBER

5c. PROGRAM ELEMENT NUMBER

6. AUTHOR(S)
Michael J. Nusca and Stephen L. Howard

5d. PROJECT NUMBER
622618H8000

5e. TASK NUMBER

5f. WORK UNIT NUMBER

U.S. Army Research Laboratory
ATTN: AMSRD-ARL-WM-BD
Aberdeen Proving Ground, MD 21005-5066

8. PERFORMING ORGANIZATION REPORT NUMBER
ARL-TR-3806

9. SPONSORING/MONITORING AGENCY NAME(S) AND ADDRESS(ES)

10. SPONSOR/MONITOR'S ACRONYM(S)

11. SPONSOR/MONITOR'S REPORT NUMBER(S)

12. DISTRIBUTION/AVAILABILITY STATEMENT
Approved for public release; distribution is unlimited.

13. SUPPLEMENTARY NOTES

14. ABSTRACT
Recent requirements for hypervelocity projectile launch for strategic U.S. Army missions have led to the proposal of a variety of gun propulsion systems. Among these systems are those that utilize solid propellant along with electrothermal-chemical (ETC) augmentation. Advanced solid propellant systems with complex grain geometry and loading configuration are also being investigated. In response to this need, the U.S. Army Research Laboratory (ARL) has, for a number of years, engaged in the study of solid propellant ignition using a hot, low molecular-weight plasma generated by ETC means. In addition, ARL is developing an ETC modeling capability using the next-generation interior ballistics code, NGEN, and a series of experimental studies in a ballistic simulator to generate code validation data. The current report demonstrates progress for application of the NGEN code to solid propellant, direct-fire gun systems in which various propellant configurations (i.e., grains and disks) are combined into a single charge in order to obtain higher-loading densities. The charge is ignited using the efflux from an ETC plasma capillary made of polyethylene. Comparison with pressure data measured in a 25-mm ballistics simulator, filled with disks of JA2 propellant as the main charge and a small amount of inert grains as filler, provides validation of the NGEN model with respect to the representation of the plasma efflux from an ablation capillary, into the chamber, and around propellant disks.

15. SUBJECT TERMS
interior ballistics, solid propellant, ignition, CFD, plasma

16. SECURITY CLASSIFICATION OF:			17. LIMITATION OF ABSTRACT	18. NUMBER OF PAGES	19a. NAME OF RESPONSIBLE PERSON
a. REPORT	b. ABSTRACT	c. THIS PAGE			Michael J. Nusca
UNCLASSIFIED	UNCLASSIFIED	UNCLASSIFIED	UL	36	19b. TELEPHONE NUMBER (*Include area code*) 410-278-6108

Standard Form 298 (Rev. 8/98)
Prescribed by ANSI Std. Z39.18

Contents

List of Figures

Acknowledgments

The U.S. Army Research Laboratory (ARL) Plasma-Propellant Interaction work unit, led by Mr. A. Williams and Dr. R. Beyer, and the ARL Multidimensional Modeling work unit, led by Dr. M. Nusca, supported this project. Drs. M. McQuaid and J. Powell (ARL) are recognized for capillary modeling. The Department of Defense Major Shared Resource Center at ARL supplied computer time for the simulations.

INTENTIONALLY LEFT BLANK.

1. Introduction

Future military engagements will require weapons systems exhibiting improved range and accuracy. One of the technologies under investigation at the U.S. Army Research Laboratory (ARL) to achieve these goals is the electrothermal-chemical (ETC) propulsion concept, shown schematically in figure 1. In the ETC gun, energy, which is stored either in batteries or a rotating device, is converted on demand into an electrically generated plasma (resulting from the ablation of polyethylene material in a capillary) that is injected into the chamber of a howitzer or gun. This plasma energy is used to ignite the chemical propulsion charge (i.e., solid propellant) as well as to enhance gun performance by taking advantage of a number of unique plasma characteristics. For example, a low density plasma jet can efficiently ignite charges of high loading density, can control propellant mass generation rates (*1*), can reduce propellant charge temperature sensitivity (i.e., the variation of gun performance with changing ambient temperature [*2*, *3*]), and can shorten ignition delay (i.e., the time interval between firing of the igniter and ignition of the propellant [*4*]). Plasma igniters replace the chemical igniter and thus enhance the safety of the gun system.

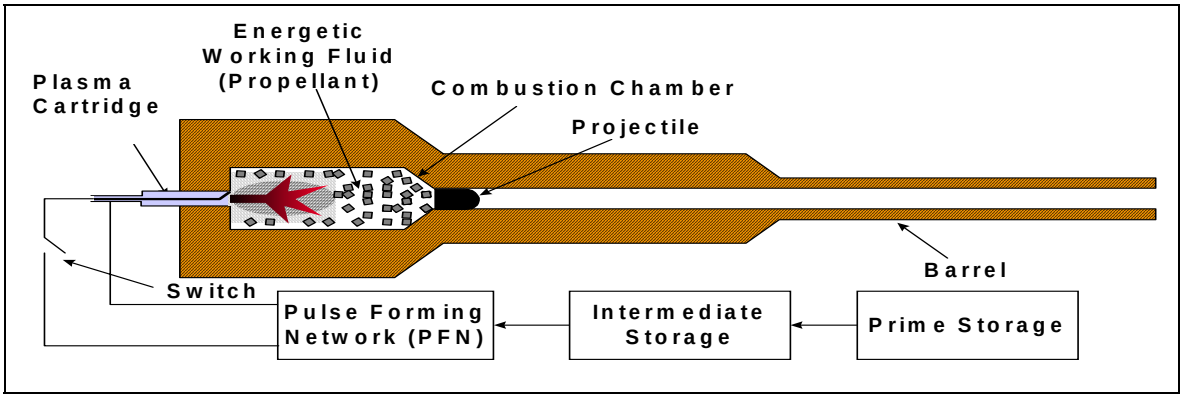

Figure 1. Electrothermal-chemical (ETC) gun concept.

Research has been carried out on the use of plasmas to ignite solid propellant (*5*, *6*). Since the plasma is at a temperature (~15,000 K) that is higher than chemical igniters (~3,000 K), the radiation properties of the plasma have also been considered. The high plasma temperature leads to radiation effects nearly 100 × greater than that of chemical igniters (i.e., a T^4 effect) (*5*). Such radiation could lead to significantly different temperature profiles within the propellant, causing changes in burn rates. In addition, plasma has a much lower density than the gases generated by a chemical igniter, a feature that alters the convective heat transfer to the propellant as the plasma moves through the grains as well as the velocity and mode of flame spreading within a propellant bed. It has been suggested that energy transport by convection may be as important as radiation transport in plasma-propellant interactions (PPIs) (*7*, *8*).

The effects previously described can lead to significant changes in ballistic behavior and useful improvements in gun performance, but an understanding of the underlying physical mechanisms is necessary in order to achieve these goals. To this end, ARL is supporting a comprehensive study of the interaction of the plasma efflux from an ETC igniter with solid propellant. The goal of this work is to elucidate the relevant physical, mechanical, and chemical mechanisms that underlie the observed ballistic effects. Various aspects of the experimental and modeling research program for PPI are described elsewhere (*9–20*). The present report explores progress in the symbiosis of experimental work and a multidimensional, multiphase interior ballistics code, NGEN, that can explicitly model the two-dimensional chamber of a gun (including chambrage), the solid propellant charge, and the inflow of plasma into the gun chamber from an ablative polyethylene capillary. The NGEN code predicts propellant ignition and flame spreading, chamber pressurization, pressure wave travel, projectile movement, and propellant burnout. The prediction of these interior ballistics parameters is important to the design of ETC guns. Code validation using data collected in a 25-mm ballistic simulator is discussed.

2. Experimental Description for the ARL 25-mm Simulator

The ARL 25-mm ETC ballistic simulator experiment, constructed by Chang and Howard (*21–23*), is used to investigate plasma flow through the center core of an assembly of concentric solid propellant disks that are each separated axially by a small gap—much like the configuration of an actual gun charge. Figure 2 shows a chamber made of visually transparent acrylic that allows cinematography of plasma flows and ignition events along the propellant bed. The chamber can withstand pressures up to ~13 MPa (1,900 psig) before rupture. Two Kistler pressure transducers (Model 211B1) are installed for monitoring chamber pressures near the breech and forward ends of the chamber. The chamber is 10.15 cm long and 3.4 cm inside diameter (ID). The chamber is narrowed to 2.44 cm diameter at the forward end and sealed. A projectile afterbody of 1.5 cm length and 2.1 cm base diameter is inserted into the forward end of the chamber. Along the length that is of constant diameter, a series of concentric disks are placed (figure 2). Initial experiments utilize disks made from the inert material Masonite* with dimensions of 33 mm outside diameter (OD), 8 mm ID, and 6.35 mm thickness (5.84 g per disk). Live propellant disks are made from graphite-free JA2 with dimensions of 33 mm OD, 9.4 mm ID, and 2.29 mm thickness (2.64 g per disk). The chambrage region surrounding the afterbody of the projectile is filled with 7-perf gr of inert material (2.54 mm in length and 2.54 mm in diameter, perforation diameter of 0.33 mm) for both inert and live experiments.

In two previous setups, 12 disks of inert material were loaded with an initial gap between each disk of about 0.8 mm, or 13 disks (last disk was 5.35 mm thick) were loaded with an initial

*Masonite is a registered trademark of Masonite International Corporation.

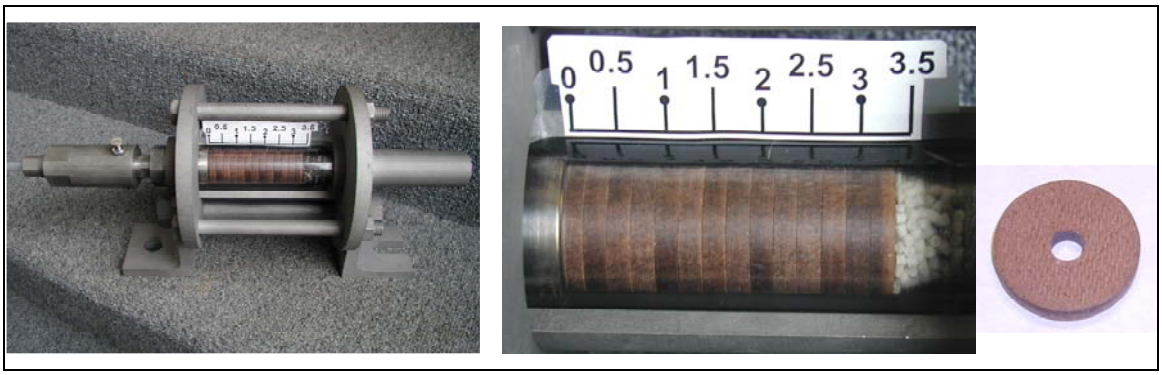

Figure 2. Photographs of the ARL 25-mm simulator loaded with disks without spacers and a single Masonite disk; dimensions shown are inches (*22*).

gap between each disk of about 0.4 mm (*21–23*). In each case, the chamber space ahead of the last disk was filled with small 7-perf gr of inert material (2.54 mm in length and 2.54 mm in diameter); a small 0.8-mm gap existed between the breech wall and the first disk and a small 0.5-mm radial gap existed along the radial wall of the chamber. These setups were used to study the performance of the NGEN code for the case of inert disks (*24*). In the latest setup, 30 graphite-free JA2 disks with a 0.5-mm gap spacing were used. This current setup is studied in the present report.

The ablative capillary used in this study to generate the plasma basically consisted of a stainless steel cylinder that housed a polyethylene tube with an ID of 3 mm. The igniter wire for the plasma was the same 0.13-mm-diameter nickel wire used in prior experiments. The anode was made of tungsten and a stainless steel cathode formed the plasma jet exit. The capillary was contained within a plasma injector which was mounted on the breech end of the chamber (see figure 2). The pulse power supply was capable of delivering energies of up to nearly 3 kJ at a voltage of 3 kV. The typical pulse length from the power supply was about 360 μs. The pulse was lengthened to ~1 μs for several experiments by the addition of a 44-mH inductor to the positive lead prior to attachment to the capillary. The voltage, current, chamber pressures, and ignition events were recorded directly on a Nicolet Integra 20 digital oscilloscope. With the measured voltage and current, the power and energy output of the capillary was subsequently calculated. These data are shown in figure 3. Typical pressure-time data recorded in the simulator are shown in figure 4.

3. NGEN Code Description

The Army's NGEN3 code is a multi-dimensional, multi-phase CFD code that incorporates three-dimensional continuum equations along with auxiliary relations into a modular code structure (*25–28*). Since accurate charge modeling involves flow field components of both a continuous

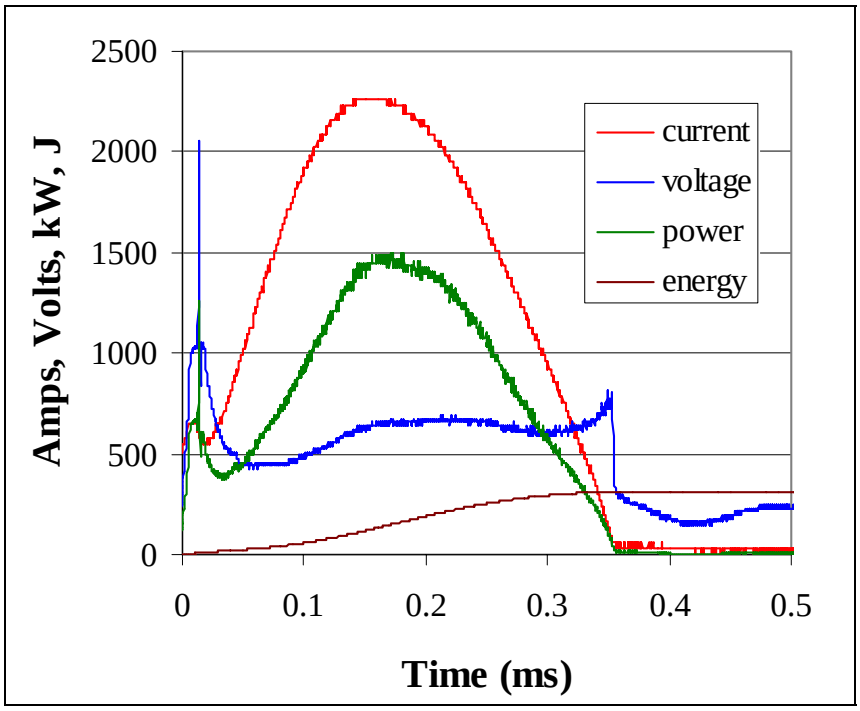

Figure 3. Electrical profiles (current in amperes: red; voltage in volts: blue; power in kilowatts: green; energy in joules: brown) used in the ARL 25-mm simulator tests (*22*).

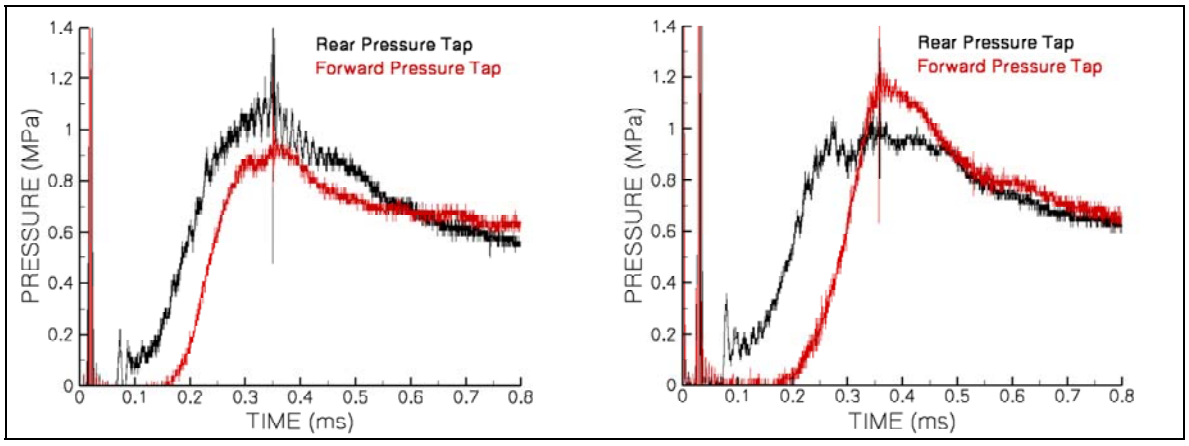

Figure 4. Pressure-time history measured in the ARL 25-mm simulator for (a) 0.4-mm disk gap shown on left and (b) 0.8-mm disk gap shown on right (*21–23*).

and a discrete nature, a coupled Eulerian-Lagrangian approach is utilized. On a sufficiently small scale of resolution in both space and time, the components of the flow are represented by the balance equations for a multicomponent reacting mixture describing the conservation of mass, momentum, and energy. A macroscopic representation of the flow is adopted using these equations derived by a formal averaging technique applied to the microscopic flow. These equations require a number of constitutive laws for closure including state equations, intergranular stresses, and interphase transfer. The numerical representation of these equations as well as the numerical solution thereof is based on a finite-volume discretization and high-order accurate, conservative numerical solution schemes. The spatial values of the dependent variables at each time step are determined by a numerical integration method denoted the Continuum Flow Solver (CFS), which treats the continuous phase and certain of the discrete phases in an Eulerian fashion. The Flux-Corrected Transport scheme (*29*) is a suitable basis for the CFS since the method is explicit and has been shown to adapt easily to massively parallel computer systems. The discrete phases are treated by a Lagrangian formulation, denoted the Large Particle Integrator (LPI), which tracks the particles explicitly and smoothes discontinuities associated with boundaries between propellants yielding a continuous distribution of porosity over the entire domain. The manner of coupling between the CFS and the LPI is through the attribution of properties (e.g., porosity, and mass generation). The size of the grid as well as the number of Lagrangian particles is user prescribed.

For the simulations of novel solid propellant configurations, such as disks stacked axially along the chamber centerline and/or thin annular concentric layers (wraps), the NGEN code takes a macroscopic approach. These solid propellant media are modeled using Lagrange particles that regress, produce combustion product gases, and respond to gas dynamic and physical forces. Individual grains, sticks, slab, and wrap layers are not resolved; rather, each medium is distributed within a specified region in the gun chamber. The constitutive laws that describe interphase drag, form-function, etc., assigned to these various media, determine preferred gas flow paths through the media (e.g., radial for disks and axial for wraps) and responses of the media to forces. Media regions can be encased in impermeable boundaries that yield to gas dynamic flow after a prescribed pressure load is reached. Details of the NGEN code are supplied elsewhere (*27*, *28*).

For modeling ETC igniters, the NGEN code is linked to the ARL plasma capillary code developed by Powell and Zielinski (*30*). This capillary code uses the length, diameter, and material composition of the ablation capillary as well as the current-time profile and supplies as output the time-dependent temperature, density, molecular weight, and flow rate of the plasma efflux. This information is mapped to the computational cells that lie along the breech face of the gun chamber, from the centerline to a predetermined radial position. Pressure is linked between the NGEN code and the capillary code so that the changing chamber pressure, as computed by the NGEN code, is input the capillary code and modifies the plasma efflux. The NGEN code represents the plasma as a single component gas with properties supplied by the

capillary code. Of course, the plasma is actually a chemically diverse and reactive media which has been treated as such in separate modeling studies (*17–19*). The macroscopic approach taken in the NGEN code, with respect to plasma representation, has been used to effectively model several solid propellant charge configurations (*24*, *31–32*).

4. Modeling Results for the ARL 25-mm Simulator

4.1 Simulations for Inert Disks

In a previous paper (*24*), the NGEN code was used to simulate the case of inert (Masonite) disks placed in the 25-mm simulator in which high temperature plasma was injected. This setup is described in the experimental description section of this report and by Nusca and Howard (*24*). Comparison between measured and computed pressure data for that work demonstrated the ability of the NGEN code to capture the plasma injection and dispersal processes within a chamber tightly loaded with propellant disks but did not test the ability of the code to simulate propellant ignition and flame spreading. Figure 5 shows the computed results (*24*) for the case of 0.4- and 0.8-mm gaps between the inert disks. These results can be compared to experimental data in figure 4 (note that a common color code has been used so that data from the pressure tap located near the breech end on the chamber are colored black and data from the pressure tap located in the chambrage region, loaded with the inert grains, are colored red). The NGEN simulations feature a pressure data station midway between the rear and the forward stations, colored green, that was not used in the simulator. Both the measured and computed pressure for the rear location show an initial rise starting before 0.1 ms and peaking at about 0.35 ms with a pressure of about 1.1 MPa. The pressure traces for the forward location show a similar behavior with a peak of about 0.9 MPa. As is expected, each pressure tap included in the simulation is affected in turn, indicative of a pressure wave that travels through the chamber from breech end

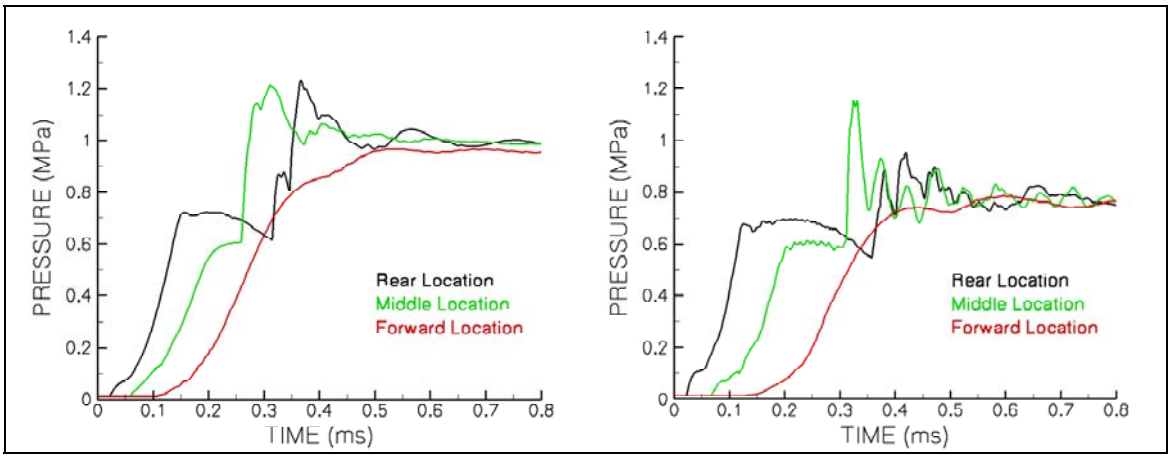

Figure 5. Computed pressure-time history for (a) 0.4-mm disk gap shown on the left and (b) 0.8-mm disk gap shown on the right (*24*).

to forward chambrage; recall from figure 3 that the peak current occurs at about 0.2 ms and that the capillary is no longer charged after about 0.38 ms. While the measured data traces show a drop in pressure to a level of about 0.6 MPa after about 0.35 ms, the computations show that the pressure in the chamber, for all tap locations, reaches a steady pressure of about 1 MPa. It is thought that some loss mechanism particular to this experiment is missing from the NGEN model or that the simulator was prone to developing leaks. To date these issues have not been specifically resolved, but it was thought that the comparisons for live propellant disks (JA2) should proceed in the current report.

4.2 Simulations for JA2 Disks

The experimental setup for the case of JA2 propellant disks loaded into the same simulator used for inert disk experiments is described in the experimental description section of this report. The NGEN code was setup as closely as possible to resemble the experiment. Figure 6 shows a series of four pulses delivered to the polyethylene capillary in order to produce four distinct plasma jets that issue into the propellant filled chamber. For a "low energy" of about 500 J (actually 260–680 J) both a short and a long pulse of about 0.3 and 1 ms, respectively, were used. For a "high energy" of about 1000 J (actually 780–1470 J) both a short and a long pulse of about 0.3 and 1 ms, respectively, were also used. These data are used in the NGEN code to form the plasma efflux into the chamber, as previously discussed.

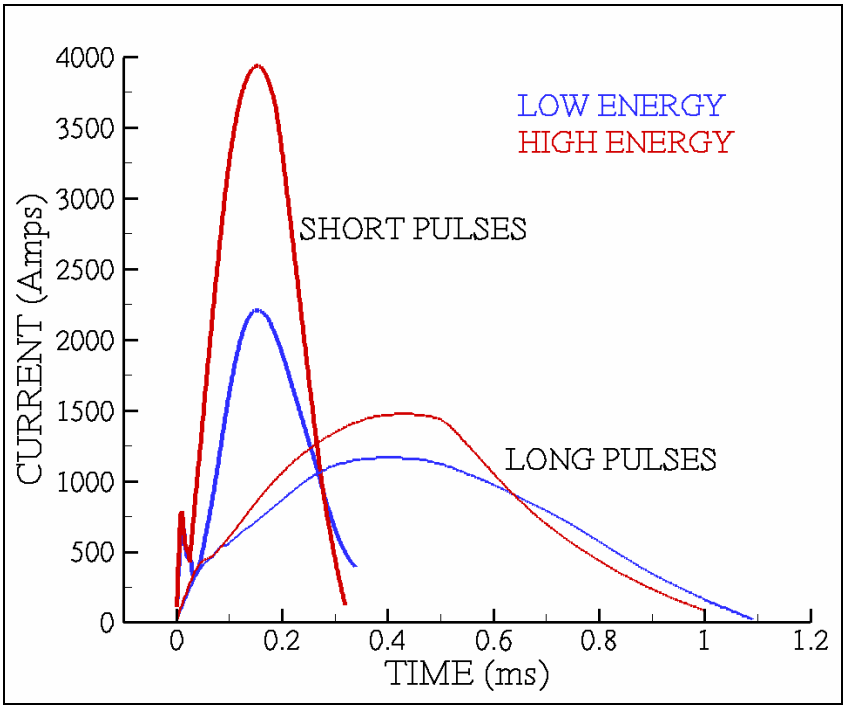

Figure 6. Experimental current profiles derived from the ARL 25-mm simulator tests and used in the NGEN code simulations.

Figure 7 shows the computed pressure results for the rear position (i.e., location of pressure tap placed along the chamber's radial wall and near the rear wall) and the forward position (i.e., location of pressure tap placed along the chamber's radial wall and into the forward chambrage) using the short duration plasma pulse with both low and high energies (values as previously described). Immediately evident is that the pressure never rises above about 3.5 MPa for the low energy pulse (figure 7a) but exceeds the yield pressure of the simulator (about 13 MPa) for the high energy pulse (figure 7b). Thus, it can be said that both the experiments and the simulations indicate that the low energy pulse is not sufficient to ignite the JA2 propellant disks, whereas the high energy pulse is more than sufficient to induce propellant ignition. For the simulations, the chamber pressure continues to rise slowly for the case of no propellant ignition because heat loss of the chamber wall is not included in the simulation and rises well above 20 MPa for the case of propellant ignition since chamber yield is also not included in the simulation. Both the computed and measured pressures for the rear position rise rapidly, followed by pressurization of the forward end of the chamber after some time delay. Both the computed and measured pressure traces show significant pressure wave action and oscillations at early times. The simulations seem to overprotect both the early-time peak pressure at the rear position and the rate at which the pressure wave reaches the forward end of the chamber. In addition, the simulations predict an earlier than measured propellant ignition (i.e., pressure runaway) for the high energy pulse (figure 7b).

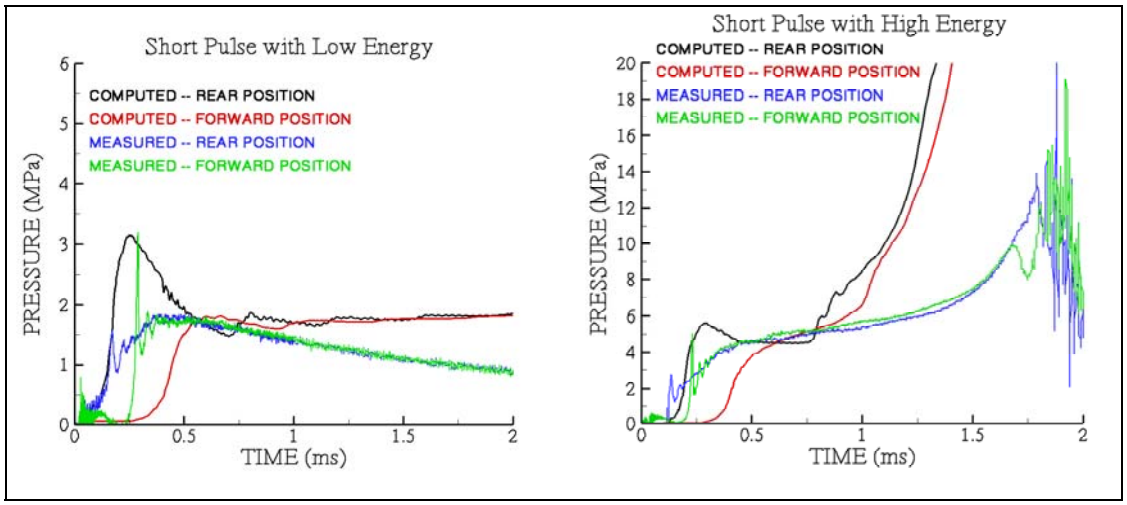

Figure 7. Pressure tap results for JA2 propellant disks in the 25-mm simulator using a short time duration current pulse (a) for the low energy pulse as shown on the left and (b) for the high energy pulse shown on the right.

Figure 8 shows the computed pressure results for the rear position and the forward position using the long duration plasma pulse with both low and high energies (values as previously described). Immediately evident is that the pressure never rises above about 4.5 MPa for the low energy pulse (figure 8a) but exceeds the yield pressure of the simulator (about 13 MPa) for the high

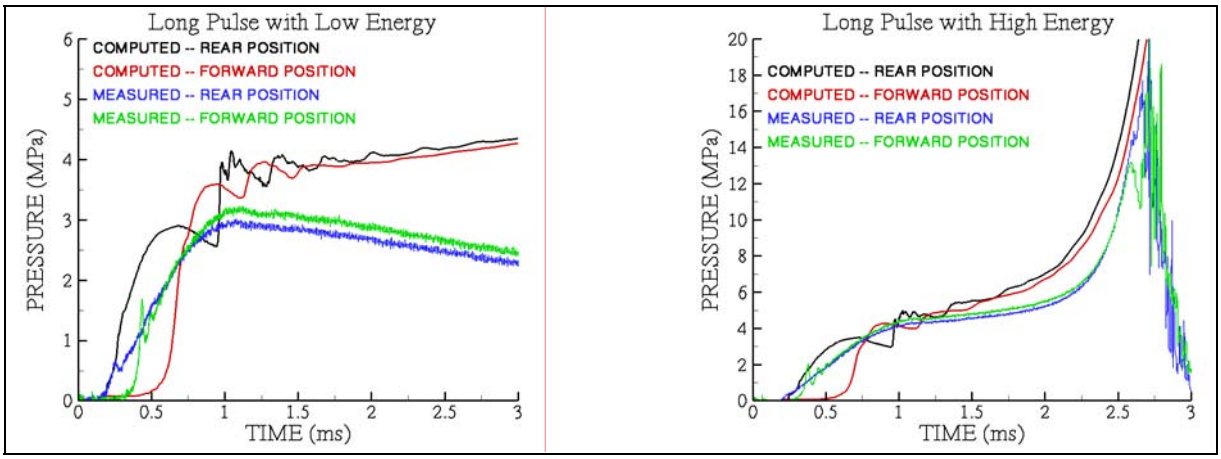

Figure 8. Pressure tap results for JA2 propellant disks in the 25-mm simulator using a long time duration current pulse (a) for the low energy pulse as shown on the left and (b) for the high energy pulse shown on the right.

energy pulse (figure 8b). Thus, it can be said that both the experiments and the simulations indicate that the low energy pulse is not sufficient to ignite the JA2 propellant disks, whereas the high energy pulse is more than sufficient to induce propellant ignition. Both the computed and measured pressures for the rear position rise rapidly, followed by pressurization of the forward end of the chamber after some time delay. Both the computed and measured pressure traces show significant pressure wave action and oscillations at early times. The simulations seem to overprotect both the early-time peak pressure at the rear position and the rate at which the pressure wave reaches the forward end of the chamber. The simulation predicts a gradual transition to propellant ignition for the high energy pulse (figure 8b) in close agreement with the measurements.

The close agreement between measured and computed pressures for the longer and more energetic plasma events would seem to indicate that physical models of the plasma properties (e.g., thermodynamic equations and the equation of state [EOS]) resident in the NGEN code require improvement. When the plasma is more slowly injected into the chamber (i.e., long duration pulse) and propellant ignition occurs the gases in the chamber are more closely simulated using a mixture of high-temperature air and reacted JA2 with relatively little plasma. Since the EOS for the plasma is probably the least accurate, the result is a more accurate overall simulation. Another explanation of the difference in behavior of the model with the results in figures 7b and 8b is the amount of energy deposited in the JA2-filled chamber as a function of pulse length. Figure 9 shows the maximum pressure for each experimental test plotted as a function of plasma energy for that particular test. For the experimental tests where insignificant JA2 combustion occurred, the pressures should be a function of the energy utilized by the plasma capillary. When these pressures are plotted as in figure 9 this function appears to be linear. When the pressures in figures 7b and 8b that occur just prior to the onset of ignition are included in figure 9, the pressure generated by the short pulse appears to be below that predicted by the

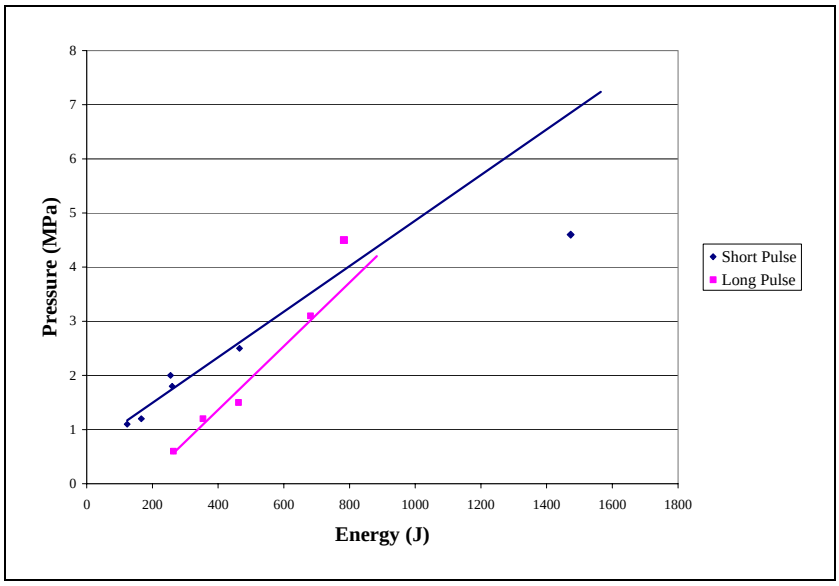

Figure 9. Plot of maximum pre-ignition pressure for 25-mm simulator filled with JA2 disks as a function of plasma energy in joules.

linear function and probably indicates that the ignition in figure 7b is weaker than expected. If the same pressure is plotted for the long pulse, it is higher than that predicted by the linear assumption. Therefore, it appears that more than sufficient energy is present for ignition in this case. The model and experiment should be somewhat in agreement as shown in figure 8b. If, in the case of the short pulse, the trend to ignition is weaker than the model is expecting, the run up to ignition in the experiment would be delayed relative to that of the model.

A more detailed examination of propellant pressurization and propellant ignition follows; the reader is directed to Nusca and Howard (*24*) for a discussion of NGEN code simulations for the case of no propellant ignition, as is the case for the low energy pulse in the current work.

Figure 10 shows a sequence of eight color flowfield pressure maps computed as part of the NGEN simulation from 0.22 to 2.5 ms for the case of a long duration current pulse of high energy, corresponding to figure 8b. A constant pressure range (i.e., blue is 0.1 MPa and below while red is 4 MPa and above) was used for the plots from 0.22 to 0.90 ms and then a larger pressure range (i.e., blue is 0.1 MPa and below while red is 12 MPa and above) was used for the plots from 0.98 to 2.5 ms. This was done because after about 1 ms the chamber is essentially of constant pressure that is steadily increasing (recall figure 8b). Superimposed on the pressure fields are velocity vectors shown in black that indicate the magnitude and direction of the gas flow (note that not all vectors are plotted for clarity). The velocity vectors illustrate that the plasma efflux is emanating from a small region along the breech wall and near the chamber centerline. It can be seen that both the empty center core of the chamber and the narrow space along the breech wall, that are not occupied by propellant, pressurize rapidly, followed by a pressure wave that moves from rear to forward through the disks (note the velocity vectors).

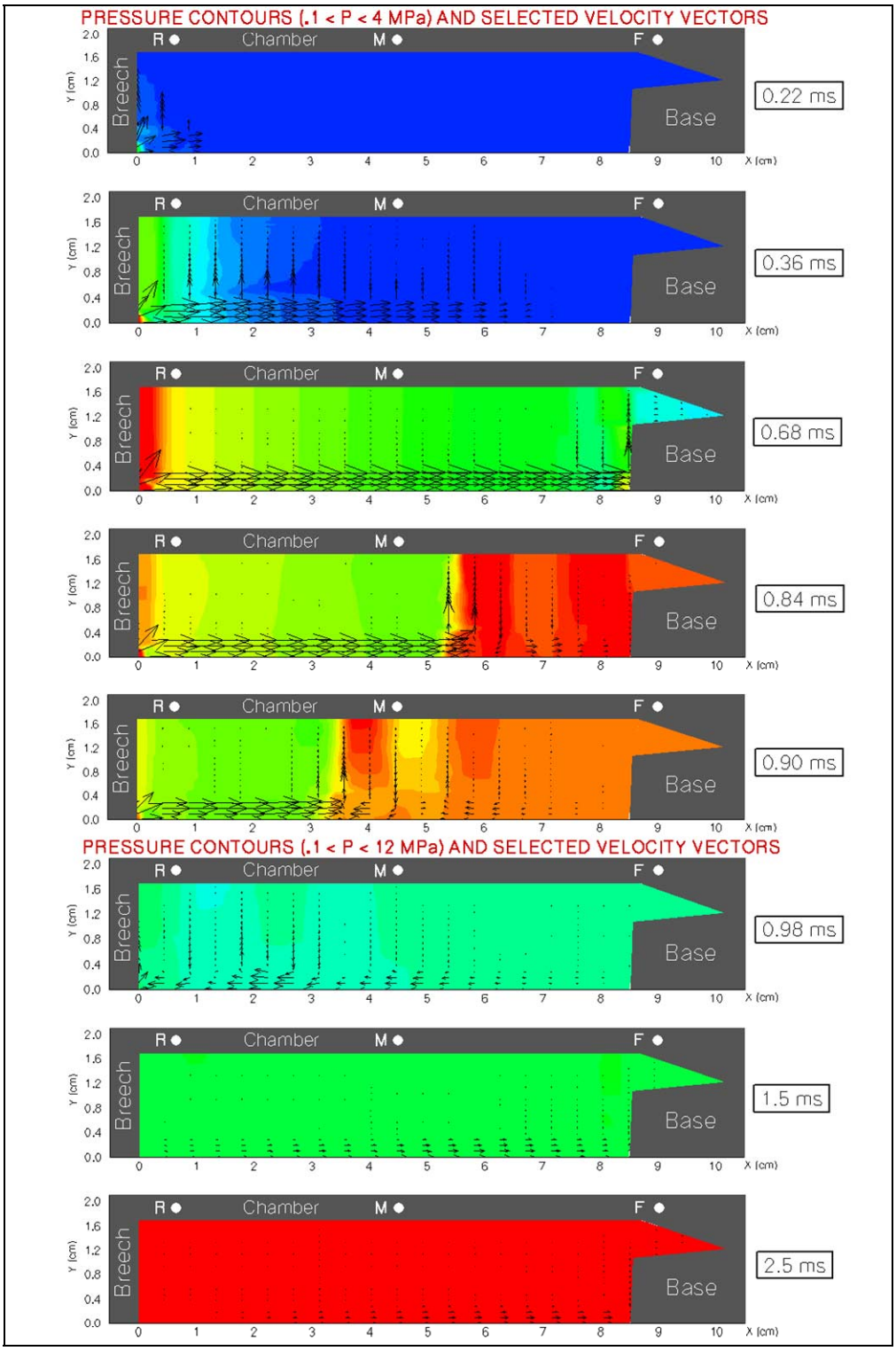

Figure 10. Color pressure contours and superimposed velocity vectors as computed using the NGEN code for the case of JA2 disks in a 25-mm simulator, long duration pulse with high energy, and for times from 0.22 to 2.5 ms.

When this wave reaches the base of the projectile afterbody (~0.68 ms), the chambrage region is pressurized, the wave reflects and then travels rearward toward the breech. By about 1 ms, the plasma efflux has terminated, most pressure wave action has ceased, and the chamber is pressurized to near uniformity. Subsequently, the chamber pressure continues to climb because the propellant disks have ignited and are generating combustion gases.

Figure 11 shows a sequence of eight color propellant temperature maps computed as part of the NGEN simulation from 0.22 to 2.5 ms for the case of a long duration current pulse of high energy, corresponding to figures 8b and 10. In this case, the color blue represents a region that is either not occupied with propellant or a region that is occupied with propellant at 294 K. The color red indicates a region of fully ignited propellant while colors between blue and red indicate propellant that is being heated but has yet to ignite. Superimposed on these fields are velocity vectors shown in black that indicate the magnitude and direction of the gas flow (note that not all vectors are plotted for clarity). The velocity vectors illustrate that the plasma efflux is emanating from a small region along the breech wall and near the chamber centerline that rapidly heats and ignites the edge of the propellant disks immediately adjacent to this efflux. As the pressure wave moves forward through the empty center core of the chamber and plasma is forced between the disks (note vectors for 0.84 ms), propellant ignition is started. Note that the inert propellant grains in the forward chambrage region are heated to ignition temperature (0.84 ms) but they are not allowed to either ignite or generate combustion gases as part of the simulation. As the pressure wave moves rearward (after 0.68 ms) the propellant disks are slowly ignited first along the edges adjacent to the chamber center core and then through the propellant as convective heat transfer is accomplished by upward moving plasma. Most wave action in the chamber ceases after 0.98 ms and the entire bed of propellant disks are fully ignited by 2.5 ms. These observations correspond to the pressure traces of figure 8b and explain the smooth and gradual rise in pressure after a steady-state is reached (i.e., pressure waves have ceased) and the propellant is ignited and generating propellant gas.

Figures 12 and 13 show a sequence of eight color flowfield pressure maps and eight color propellant temperature maps, respectively, computed as part of the NGEN simulation from 0.22 to 2.5 ms for the case of a long duration current pulse of low energy (see figure 8a). A constant pressure range (i.e., blue is 0.1 MPa and below while red is 4 MPa and above) was used in figure 12 for plots from 0.22 to 0.90 ms and then a larger pressure range (i.e., blue is 0.1 MPa and below while red is 12 MPa and above) was used for the plots from 0.98 to 2.5 ms. For figure 13, the color blue represents a region that is either not occupied with propellant or a region that is occupied with propellant at 294 K, while the color red indicates a region of fully ignited propellant; colors between blue and red indicate propellant that is being heated but has yet to ignite. Superimposed on the pressure and temperature fields are velocity vectors shown in black that indicate the magnitude and direction of the gas flow (note that not all vectors are plotted for clarity).

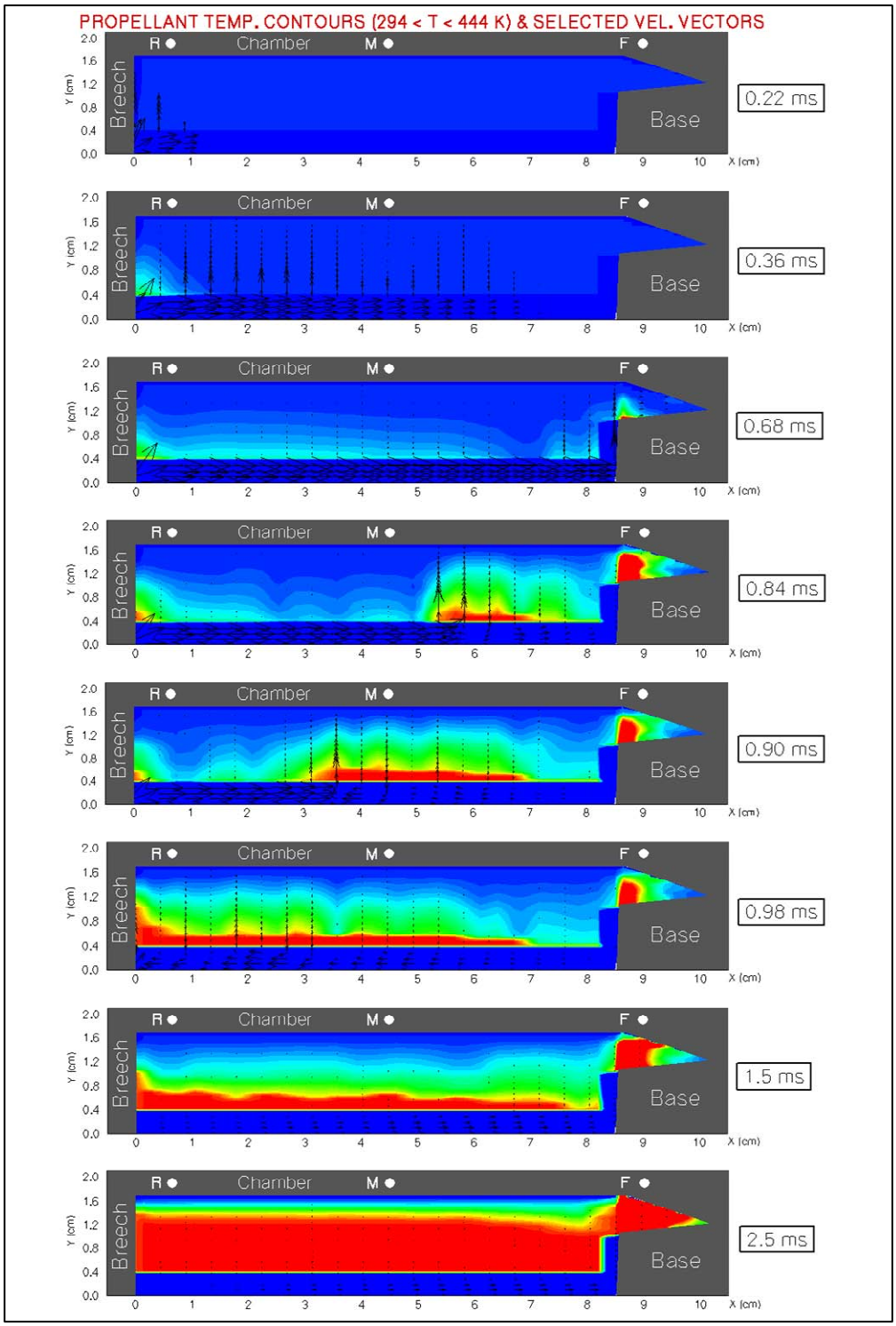

Figure 11. Color propellant temperature contours and superimposed velocity vectors as computed using the NGEN code for case of JA2 disks in simulator, long duration pulse with high energy, and for times from 0.22 to 2.5 ms.

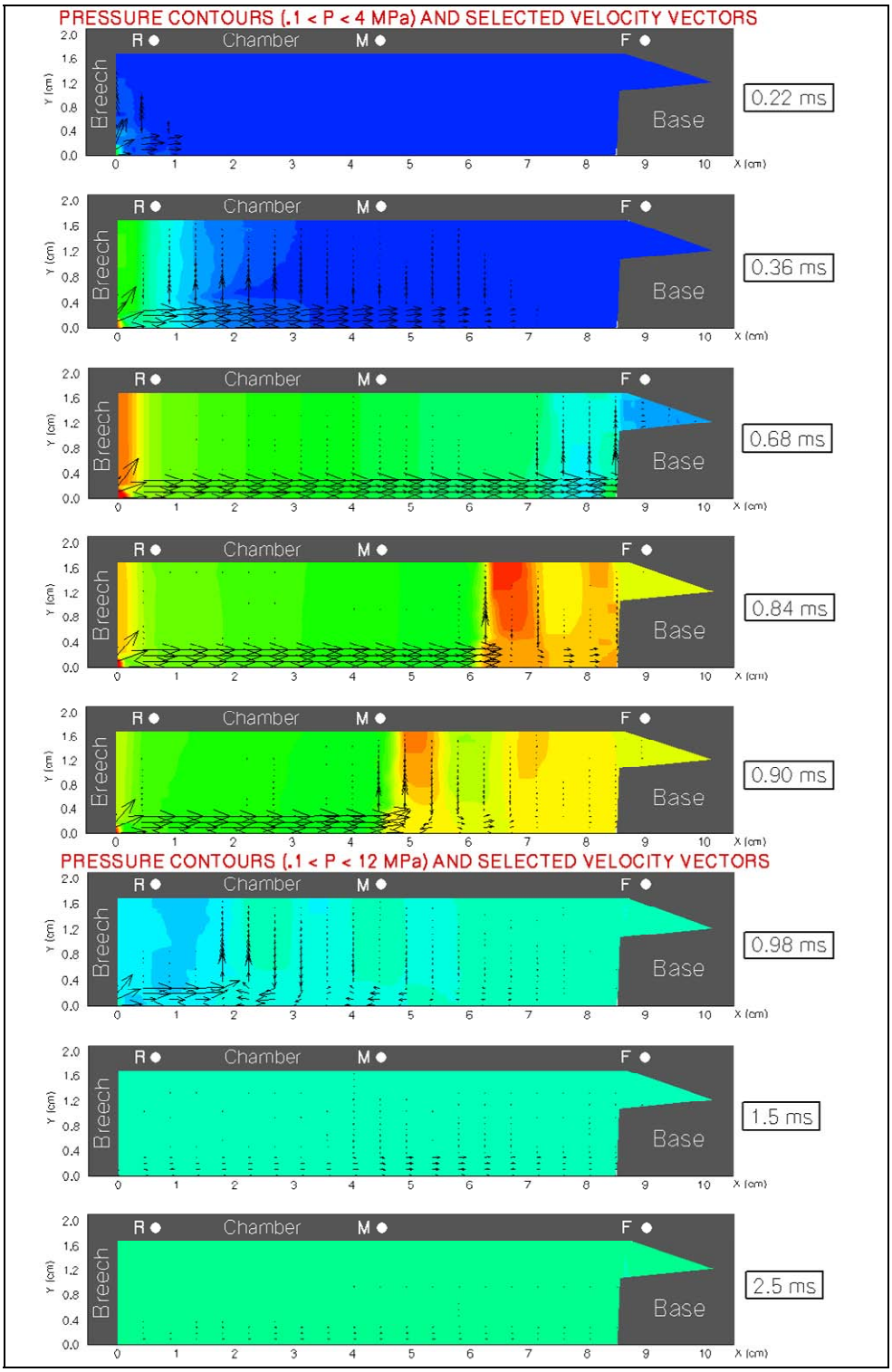

Figure 12. Color pressure contours and superimposed velocity vectors as computed using the NGEN code for the case of JA2 disks in a 25-mm simulator, long duration pulse with low energy, and for times from 0.22 to 2.5 ms.

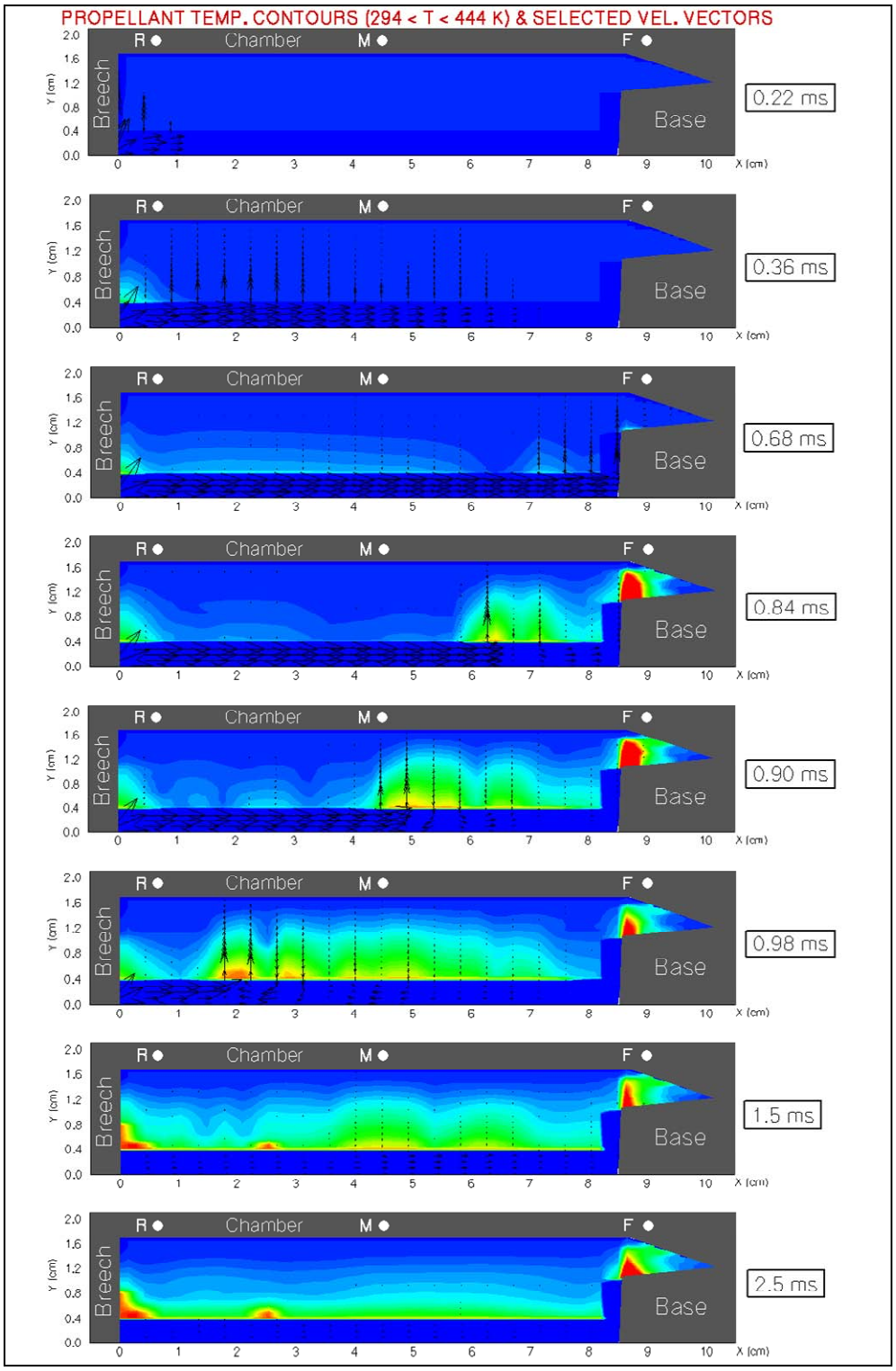

Figure 13. Color propellant temperature contours and superimposed velocity vectors as computed using the NGEN code for case of JA2 disks in simulator, long duration pulse with low energy, and for times from 0.22 to 2.5 ms.

Comparing the results of the high energy pulse (figures 10 and 11) to those for the low energy pulse (figures 12 and 13), it can be observed that after the plasma efflux ceases (i.e., after about 0.98 ms) a high energy pulse causes propellant ignition while the low energy pulse does not. For the low energy pulse, pressure levels between the disk propellant, especially in the forward section of the chamber are too low to create enough convective heat transfer into the propellant for ignition, suggesting that a link exists between the energy content of the plasma and propellant ignition which is similar to the case of conventional hot gas igniters. It is clear that the presence of plasma, per se, does not guarantee propellant ignition, but that the plasma efflux must be sufficiently energetic regardless of the duration.

These points are reinforced by the results displayed in figures 14 and 15, showing a sequence of eight color propellant temperature maps computed as part of the NGEN simulation from 0.22 to 2.5 ms for the case of a short duration current pulse of either high or low energy, respectively (recall figure 7). The high energy pulse of short duration rapidly ignites the propellant charge (even more rapidly than the same pulse but of long duration [figure 11]) while the low energy pulse or short duration merely heats the edge of the propellant disks and fails to effectively penetrate the charge.

5. Summary and Conclusions

The NGEN multidimensional, multiphase CFD code has been successfully used to model the interior ballistics of solid propellant charges ignited using hot chemical gases like those generated by burning black powder or Benite (*27*, *28*). In order to model charges ignited using injected plasma, which is generated by an ablation capillary of polyethylene, the NGEN code was upgraded with a single-component, non-reacting gas phase treatment of the plasma and linked to a well-known and independently validated capillary model.

In previous works, NGEN simulations for plasma injection into the gun chamber showed that the ignition delay is lengthened, even to the point of a non-ignition event, when the current that is input to the ablation capillary is reduced (*24*, *31*, *32*). This is an important result as it necessitates a closer linkage between the charge designer and the igniter designer when the ETC option is utilized. Given independent plasma-propellant modeling results that point to the need for a multicomponent, reacting flow representation of the plasma (*17–19*) and the incompatibility of this level of plasma modeling with the NGEN code, within the constraints of currently available computers, there is an immediate need to validate the NGEN code for the design of ETC guns.

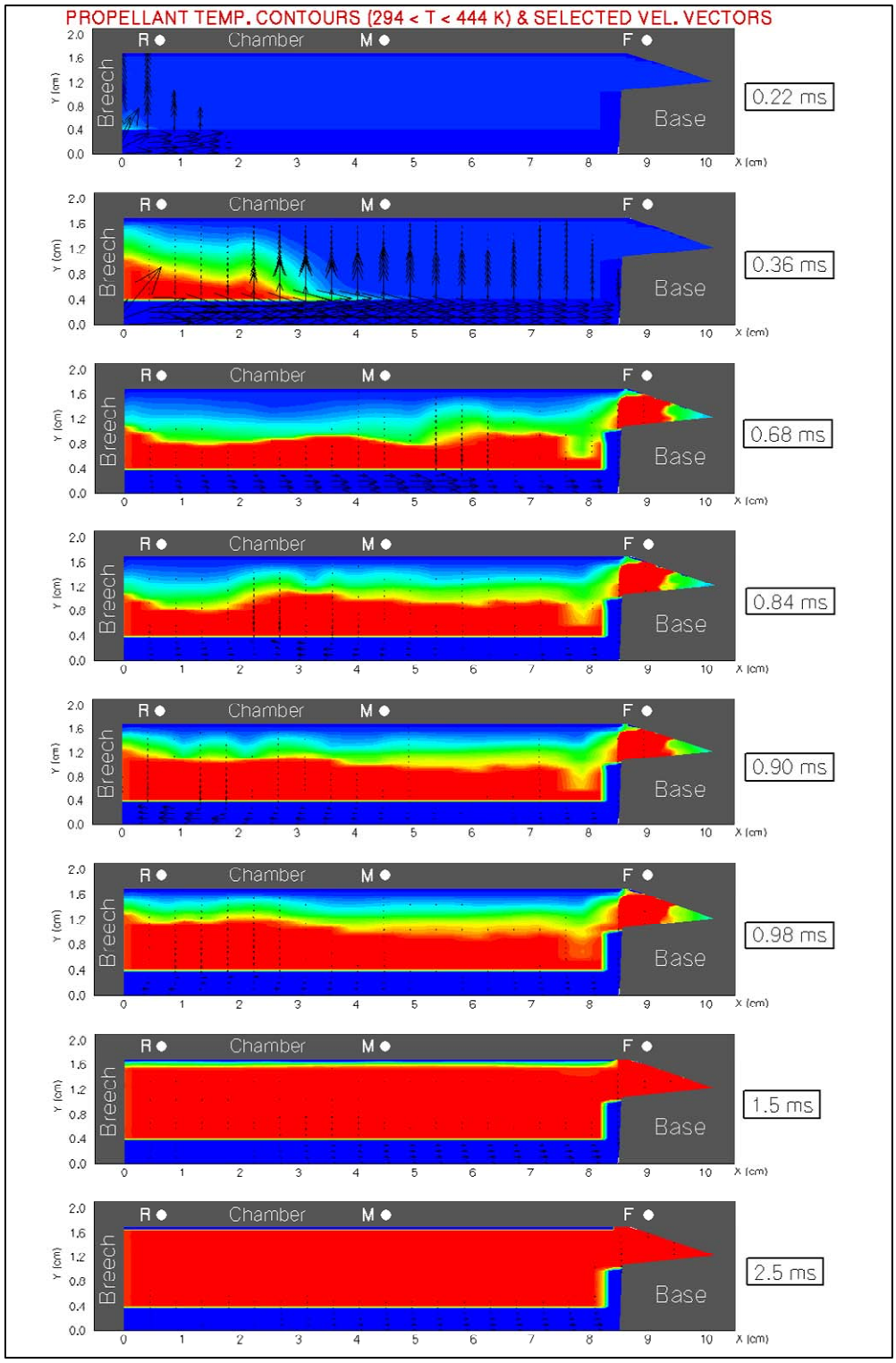

Figure 14. Color propellant temperature contours and superimposed velocity vectors as computed using the NGEN code for case of JA2 disks in simulator, short duration pulse with high energy, and for times from 0.22 to 2.5 ms.

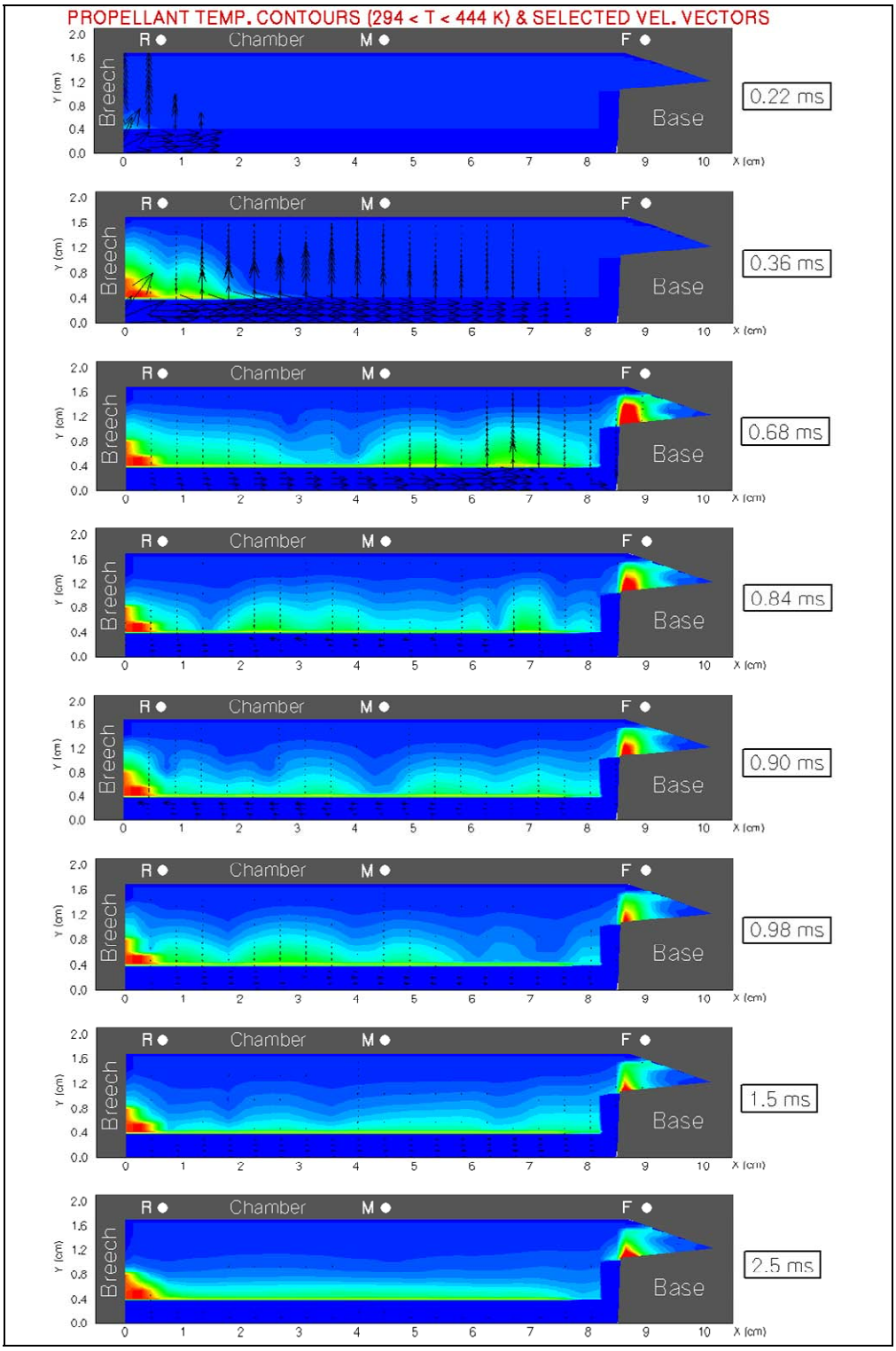

Figure 15. Color propellant temperature contours and superimposed velocity vectors as computed using the NGEN code for case of JA2 disks in simulator, short duration pulse with low energy, and for times from 0.22 to 2.5 ms.

A significant step in this effort has been to compare the chamber pressure measured in a sub-scale ballistic simulator with that computed using the code. The configuration chosen was a 25-mm chamber filled with either inert disks or disks made from JA2 propellant and linked to an ablative capillary of the size and power of a typical ETC gun igniter. Previous works showed that the NGEN code was able to capture the essential features of the plasma efflux as it was injected and then spread around the inert disks via diffusion/convection (*24*). In the present work, using a chamber filled with JA2 disks, the NGEN code results showed that a low energy pulse (500 J), whether short (~0.3 ms) or long (~1 ms) in duration, was not sufficient to ignite the disks, while a high energy pulse (1000 J) of either duration was able to accomplish JA2 ignition. These results are in full agreement with the experiment. Detailed comparison between the measured and computed pressure histories showed some discrepancies that have been attributed to the state equations employed by the model and/or an apparent ignition "threshold" in terms of plasma energy that may have biased the comparison. A remarkable agreement between measured and computed pressure history was achieved for the case of a long duration pulse and high energy.

6. References

1. Del Güercio, M. Propellant Burn Rate Modification by Plasma Injection. *Proceedings of the 34th JANNAF Combustion Meeting*, CPIA Publication 662, 1997; *1*, 35–42.

2. Perelmutter, L.; Sudai, M.; Goldenberg, C.; Kimhe, D.; Zeevi, Z.; Arie, S.; Melnik, M.; Melnik, D. Temperature Compensation by Controlled Ignition Power in SPETC Guns. *Proceedings of the 16th International Symposium on Ballistics*, 1996; 145–152.

3. Dyvik, J. A.; Katulka, G. ETC Temperature Compensation; Experimental Results of 120-mm Test Firings. *Proceedings of the 33rd JANNAF Combustion Meeting*, CPIA Publication 653, 1996; *3*, 111–119.

4. Katulka, G. L.; Dyvik, J. Experimental Results of Electrical Plasma Ignition in 120-mm Solid Propellant Tank Gun Firings. *Proc. 33rd JANNAF Combustion Meeting*, CPIA Publication 653, 1996; *3*, 103–110.

5. White, K. J.; Katulka, G. L.; Khuan, T.; Nekula, K. *Plasma Characterization for Electrothermal-Chemical (ETC) Gun Applications*; ARL-TR-1491; U.S. Army Research Laboratory: Aberdeen Proving Ground, MD, September 1997.

6. Perelmutter, L.; Goldenberg, C.; Sudai, M.; Alimi, R.; Furman, M.; Kimhe, D.; Appelbaum, G.; Arie, S.; Zeevi, Z.; Melnik, D. Experimental Study of Plasma Propagation and Ignition of Solid Propellant in a Gun Chamber. *Proceedings of the 16th International Symposium on Ballistics*, September 1996.

7. Nusca, M. J.; White, K. J. Plasma Radiative and Convective Interactions with Propellant Beds. *Proceedings of the 34th JANNAF Combustion Meeting*, CPIA Publication 662, 1997; *1*, 21–42.

8. White, K. J.; Williams, A. W.; Nusca, M. J. Plasma Output and Propellant Radiation Absorption Characteristics. *Proceedings 35th JANNAF Combustion Meeting*, CPIA Publication 680, 1998; *1*, 237–246.

9. Kaste, P. J.; Birk, A.; Del Güercio, M. A.; Lieb, R.; Kinkennon, A. Surface Phenomena of Plasma-Treated Propellant Samples. *Proc. of the 36th JANNAF Combustion Meeting*, CPIA Publication 691, 1999; *2*, 77–98 (see also ARL-TR-2500; U.S. Army Research Laboratory: Aberdeen Proving Ground, MD, May 2001).

10. Williams, A. W.; White, K. J. Plasma-Propellant Interaction Studies: Measurements of In-Depth Propellant Heating by Plasma Radiation; Investigation of Possible Plasma-Induced Propellant Erosion. *Proceedings of the 36th JANNAF Combustion Meeting*, CPIA Publication 691, 1999; *2*, 67–76.

11. Beyer, R. A. Small Scale Experiments in Plasma Propellant Interactions. *Proc. of the 37th JANNAF Combustion Subcommittee Meeting*, CPIA Publication 701, 2000; *1*, 137–144.

12. Fifer, R. A.; Sagan, E. S.; Beyer, R. A. Investigation of the Role of Plasma Chemistry in the Plasma Propellant Interaction Process. *Proc. of the 38th JANNAF Combustion Subcommittee Meeting*, April 2002.

13. Litzinger, T. A.; Li, J-Q.; Kwon, J.; Thynell, S. Experimental Investigations of the Characteristics of Electrothermal-Chemical Plasma. *Proc. of the 38th JANNAF Combustion Subcommittee Meeting*, April 2002.

14. Chang, L-M.; Beyer, R. A.; Howard, S. L. Characterization of Plasma Jet Flows and their Interaction with Propelling Charges. *Proceedings of the 38th JANNAF Combustion Subcommittee Meeting*, CPIA Publication 712, 2002; *1*, 299–307.

15. McQuaid, M. J.; Nusca, M. J. Calculating the Chemical Compositions of Plasmas Generated by an Ablating-Capillary Arc Ignition System. *Proc. of the 36th JANNAF Combustion Meeting*, CPIA Publication 691, 1999; *2*, 143–158 (see also ARL-TR-2046; U.S. Army Research Laboratory: Aberdeen Proving Ground, MD, 1999).

16. McQuaid, M. J.; Nusca, M. J. Thermodynamic Property Characterization of Plasmas Generated by an Ablating-Capillary Arc. *Proc. of the 37th JANNAF Combustion Subcommittee Meeting*, CPIA Publication 701, 2000; *1*, 157–166 (see also ARL-TR-2427; U.S. Army Research Laboratory: Aberdeen Proving Ground, MD, May 2001).

17. Nusca, M. J.; McQuaid, M. J.; Anderson, W. R. Numerical Model of them Plasma Jet Generated by an Electrothermal-Chemical Igniter. *Journal of Thermophysics and Heat Transfer* **2002**, *16* (1), 44–52.

18. Nusca, M. J.; Anderson, W. R.; McQuaid, M. J. *Multispecies Reacting Flow Model for the Plasma Efflux of an ETC Igniter – Application to an Open-Air Plasma Jet Impinging on an Instrumented Probe*; ARL-TR-3227; U.S. Army Research Laboratory: Aberdeen Proving Ground, MD, July 2004.

19. Nusca, M. J.; Anderson, W. R.; McQuaid, M. J. *Multispecies Reacting Flow Model for the Πλασμα Efflux of an ETC Igniter – Application to an Open-Air Plasma Jet Impinging on an Instrumented Plate*; ARL-TR-3275; U.S. Army Research Laboratory: Aberdeen Proving Ground, MD, August 2004.

20. Anderson, W. R.; Schroeder, M. A. Chemical Mechanism for ETC Plasma Interaction with Air. *Proceedings of the 36th JANNAF Combustion Meeting*, CPIA Publication 691, 1999; *2*, 43–54.

21. Chang, L. M. *Interior Ballistic Simulations of 25-mm Gun Charges*; BRL-TR-3330; U.S. Army Ballistic Research Laboratory: Aberdeen Proving Ground, MD, 1992.

22. Chang, L. M.; Howard, S. L. Characterization of Plasma Jet Flows and Their Interaction With Propelling Charges. *Proceedings of 20th International Symposium on Ballistics*, 2002; *1*, 392–400.

23. Chang, L. M.; Howard, S. L. Characterization of Flame Propagation in Narrow Channels of Disc Propellant Charges with Plasma Ignition. *Proceedings of the 51st JANNAF Propulsion Meeting*, CPIA Publication JPMCD02, November 2002.

24. Nusca, M. J.; Howard, S. L. Modeling Plasma Flow in Solid Propellant Charges Using the NGEN Multiphase CFD Code. *Proceedings of the 40th JANNAF Combustion Subcommittee Meeting*, CPIA Publication JSC CD-39, June 2005 (see also ARL-TR-3768; U.S. Army Research Laboratory: Aberdeen Proving Ground, MD, April 2006).

25. Gough, P. S. Modeling Arbitrarily Packaged Multi-Increment Solid Propellant Charges of Various Propellant Configurations. *Proc. of the 33rd JANNAF Combustion Meeting*, CPIA Publication 653, 1996; *1*, 421–435.

26. Gough, P. S. Extensions to the NGEN Code: Propellant Rheology and Container Properties. *Proceedings of the 34th JANNAF Combustion Meeting*, CPIA Publication 662, 1997; *3*, 265–281.

27. Nusca, M. J.; Gough, P. S. Numerical Model of Multiphase Flows Applied to Solid Propellant Combustion in Gun Systems, AIAA Paper No. 98-3695; July 1998.

28. Nusca, M. J. *High-Performance Computing and Simulation for Advanced Armament Propulsion*; ARL-TR-3215; U.S. Army Research Laboratory: Aberdeen Proving Ground, MD, June 2004.

29. Boris, J. P.; et al. *LCPFCT – A Flux-Corrected Transport Algorithm for Solving Generalized Continuity Equations*; NRL-MR/6410-93-7192; U.S. Naval Research Laboratory: Washington, DC, April 1993.

30. Powell, J. D.; Zielinski, A. E. *Theory and Experiment for an Ablating-Capillary Discharge and Application to Electrothermal-Chemical Guns*; BRL-TR-3355; U.S. Army Ballistic Research Laboratory: Aberdeen Proving Ground, MD, 1992.

31. Conroy, P. J.; Nusca, M. J. *Progress in the Modeling of High-Loading Density Direct-Fire Charges Using the NGEN Multiphase CFD Code*; ARL-TR-2934; U.S. Army Research Laboratory: Aberdeen Proving Ground, MD, March 2003 (see also *Proceedings of the 38th JANNAF Combustion Meeting*, CPIA Publication 712, 2002; *2*, 449–462).

32. Nusca, M. J. Numerical Simulation of Plasma Ignition for High-Loading Density Charges in an ETC Sun Using the NGEN Code. *Proceedings of the 39th JANNAF Combustion Meeting*, CPIA Publication JSC CD-25, December 2003.

NO. OF COPIES	ORGANIZATION
1 (PDF ONLY)	DEFENSE TECHNICAL INFORMATION CTR DTIC OCA 8725 JOHN J KINGMAN RD STE 0944 FORT BELVOIR VA 22060-6218
1	US ARMY RSRCH DEV & ENGRG CMD SYSTEMS OF SYSTEMS INTEGRATION AMSRD SS T 6000 6TH ST STE 100 FORT BELVOIR VA 22060-5608
1	INST FOR ADVNCD TCHNLGY THE UNIV OF TEXAS AT AUSTIN 3925 W BRAKER LN AUSTIN TX 78759-5316
1	DIRECTOR US ARMY RESEARCH LAB IMNE ALC IMS 2800 POWDER MILL RD ADELPHI MD 20783-1197
3	DIRECTOR US ARMY RESEARCH LAB AMSRD ARL CI OK TL 2800 POWDER MILL RD ADELPHI MD 20783-1197

ABERDEEN PROVING GROUND

1	DIR USARL AMSRD ARL CI OK TP (BLDG 4600)

NO. OF COPIES ORGANIZATION

1 DIRECTOR
US ARMY RESEARCH LAB
AMSRD ARL D
J MILLER
2800 POWDER MILL RD
ADELPHI MD 20783-1197

3 DIRECTOR
US ARMY RESEARCH LAB
AMSRD ARL RO P
D MANN
R SHAW
TECH LIB
PO BOX 12211
RESEARCH TRIANGLE PARK NC
27709-2211

8 US ARMY AVIATN & MSLE CMD
AMSRD AMR PS PT
W CHEW
C DOLBEER
J S LILLY
M LYON
J M FISHER
B P MARSH
R S MICHAELS
D THOMPSON
REDSTONE ARSENAL AL
35898-5249

2 PM MAS
SFAE AMO MAS
LTC M BUTLER
PICATINNY ARSENAL NJ
07806-5000

2 PM CAS
SFAE AMO CAS
PICATINNY ARSENAL NJ
07806-5000

8 DIR BENET WEAPONS LAB
M AUDINO
R DILLON
R FISCELLA
R HASENBEIN
E KATHE
J MCNEIL
K MINER
S SOPOK
WATERVLIET NY 12189-4000

NO. OF COPIES ORGANIZATION

17 CDR US ARMY ARDEC
D CARLUCCI
R CARR
R CIRINCIONE
S EINSTEIN
T GORA
P HUI
J LANNON
E LOGSDEN
P LU
B MACHAK
S NICHOLICH
P O'REILLY
J O'REILLY
J RUTKOWSKI
A SABASTO
J SHIN
R SURAPANENI
PICATINNY ARSENAL NJ 07806-5000

1 CDR
RADFORD ARMY AMMO PLANT
SMCAR QA HI LIB
RADFORD VA 24141-0298

1 COMMANDANT
USAFC&S
ATSF CN P GROSS
FT SILL OK 73503-5600

2 CDR NAVAL RSRCH LAB
TECH LIB
J BORIS
WASHINGTON DC 20375-5000

1 OFFICE OF NAVAL RSRCH
J GOLDWASSER
875 N RANDOLPH ST RM 653
ARLINGTON VA 22203-1927

6 CDR
NAVAL SURFACE WARFARE CTR
R2A R DOHERTY
TM3 C GOTZMER
R22 C MICHIENZI
OPA S MITCHELL
R3A S C SMITH
TECH LIB
INDIAN HEAD MD 20640-5000

NO. OF COPIES ORGANIZATION

5 CDR
NAVAL SURFACE WARFARE CTR
J FRAYSEE G33
R FRANCIS T08
T C SMITH
T TSCHIRN G30
TECH LIB
DAHLGREN VA 22448-5000

3 CDR
NAVAL AIR WARFARE CTR
A ATWOOD
S BLASHILL
T PARR
CHINA LAKE CA 93555-6001

1 AIR FORCE RSRCH LAB
MNME EN MAT BR
B WILSON
2306 PERIMETER RD
EGLIN AFB FL 32542-5910

1 AIR FORCE OFC OF SCI RSRCH
M BERMAN
875 N RANDOLPH ST
STE 235 RM 3112
ARLINGTON VA 22203-1768

1 NASA LANGLEY RSRCH CENTER
D BUSHNELL
MS 110
HAMPTON VA 23681-2199

1 DIR SANDIA NATL LABS
M BAER DEPT 1512
PO BOX 5800
ALBUQUERQUE NM 87185

2 DIR LAWRENCE LIVERMORE NL
L FRIED
M MURPHY
PO BOX 808
LIVERMORE CA 94550-0622

1 CENTRAL INTELLIGENCE AGNCY
J BACKOFEN
RM 4PO7 NHB
WASHINGTON DC 20505

1 BATTELLE EAST SCI & TECH
A ELLIS
1204 TECHNOLOGY DR
ABERDEEN MD 21001-1228

NO. OF COPIES ORGANIZATION

2 JHU CHEM PROP INFO AGNCY
W HUFFERD
R FRY
10630 LITTLE PATUXENT PKWY
STE 202
COLUMBIA MD 21044-3200

1 OUSD (AT&L)/STRAT & TACT
SYS MUNITIONS
T MELITA
3090 DEFENSE PENTAGON
RM 3B1060
WASHINGTON DC 20301-3090

1 BRIGHAM YOUNG UNIV
DEPT OF CHEMICAL ENGRG
M BECKSTEAD
PROVO UT 84601

1 CALIF INSTITUTE OF TECHLGY
F E C CULICK
204 KARMAN LAB
MS 301 46
1201 E CALIFORNIA ST
PASADENA CA 91109

2 UNIV OF ILLINOIS
DEPT OF MECH INDUSTRY
ENGINEERING
H KRIER
R BEDDINI
144 MEB 1206 N GREEN ST
URBANA IL 61801-2978

5 PENNSYLVANIA STATE UNIV
DEPT OF MECHANICAL ENGRG
K KUO
T LITZINGER
G SETTLES
S THYNELL
V YANG
UNIVERSITY PARK PA 16802-7501

1 ARROW TECHLGY ASSOC INC
1233 SHELBURNE RD D 8
SOUTH BURUNGTON VT 05403

NO. OF COPIES	ORGANIZATION
2	ALLIANT TECH SYS INC E LYNAM WV01 G CORLEY WV01 PO BOX 210 ROCKET CENTER WV 26726
3	ALLIANT TECH SYS INC C AAKHUS MN07 LW54 R DOHRN MN07LW54 D KAMDAR MN07 LW54 5050 LINCOLN DR EDINA MN 55436
2	ALLIANT TEC SYS INC RADFORD ARMY AMMO PLANT W J WORRELL VA02 ROUTE 114 PO BOX 1 RADFORD VA 24141
4	ATK THIOKOL P BRAITHWAITE T B FARABAUGH W B WALKUP R WARDLE PO BOX 707 BRIGHAM CITY UT 84302-0707
1	ATK ELKTON J HARTWELL PO BOX 241 ELKTON MD 21921-0241
1	BAE ARMAMENT SYS DIV JAHN DYVIK 4800 E RIVER RD MINNEAPOLIS MN 55421-1498
2	GEN DYNAMICS ORD/TACT SYS N HYLTON J BUZZETT 10101 DR M L KING ST N ST PETERSBURG FL 33716
3	GENERAL DYNAMICS ST MARKS J DRUMMOND H RAINES D W WORTHINGTON PO BOX 222 SAINT MARKS FL 32355-0222
1	GENERAL DYNAMICS ARM SYS J TALLEY 128 LAKESIDE AVE BURLINGTON VT 05401
1	PAUL GOUGH ASSOC INC P S GOUGH 1048 SOUTH ST PORTSMOUTH NH 03801-5423
3	VERITAY TECHGY INC R SALIZONI J BARNES E FISHER 4845 MILLERSPORT HWY EAST AMHERST NY 14501-0305
1	SRI INTERNATIONAL PROPULSION SCIENCES DIV TECH LIB 333 RAVENWOOD AVE MENLO PARK CA 94025-3493
1	NETWORKING COMPUTING SVCS S RAY 1200 WASHINGTON AVE S MINNEAPOLIS MN 55415

NO. OF
COPIES ORGANIZATION

ABERDEEN PROVING GROUND

1 CDR USAATC
CSTE DTC AT SL
APG MD 21005

66 DIR USARL
AMSRD ARL WM
T ROSENBERGER
AMSRD ARL WM M
S MCKNIGHT
AMSRD ARL WM T
B BURNS
AMSRD ARL WM TB
P BAKER
AMSRD ARL WM B
C CANDLAND
J MORRIS
J NEWILL
M ZOLTOSKI
AMSRD ARL WM BA
B DAVIS
G BROWN
D HEPNER
G KATULKA
T KOGLER
D LYON
AMSRD ARL WM BC
M BUNDY
G COOPER
J DESPIRITO
J GARNER
P PLOSTINS
J SAHU
S SILTON
P WEINACHT
AMSRD ARL WM BD
W ANDERSON
R BEYER
A BRANT
S BUNTE
L CHANG
T COFFEE
J COLBURN
P CONROY
N ELDREDGE
B FORCH
B HOMAN
A HORST
S HOWARD (6 CPS)
P KASTE
A KOTLAR
C LEVERITT
R LIEB

NO. OF
COPIES ORGANIZATION

K MCNESBY
M MCQUAID
A MIZIOLEK
J NEWBERRY
M NUSCA (6 CPS)
R PESCE-RODRIGUEZ
S PIRIANO
G REEVES
B RICE
R SAUSA
J SCHMIDT
A WILLIAMS
AMSRD ARL WM BF
R ANDERSON
W OBERLE
D WILKERSON
AMSRD ARL WM EG
E SCHMIDT
AMSRD ARL WM SG
W CIEPIELA

INTENTIONALLY LEFT BLANK.